Journal of Chemical Ecology, Vol. 13, No. 3, 1987

QUANTITATIVE COMPARISON OF BEHAVIORAL AND NEUROPHYSIOLOGICAL RESPONSES OF INSECTS TO ODORANTS: Inferences about Central Nervous System Processes

M.S. MAYER, R.W. MANKIN, and A.J. GRANT[1]

Insect Attractants, Behavior, and Basic Biology Research Laboratory
Agricultural Research Service, U.S. Department of Agriculture
Gainesville, Florida 32604

(Received February 19, 1985; accepted March 31, 1986)

Abstract—A consistent pattern of relationships emerges from comparisons of insect electroantennograms, peripheral olfactory receptor neuron responses, and behavioral responses to quantified concentrations of odorants. One consistency is that all of the different response measurements can be described by stimulus–response curves of the same form. Another is that the responses have characteristic groupings when they are plotted against odorant concentration. The pattern of relationships is exemplified in the responses of *Trichoplusia ni* (Hübner), *Heliothis zea* (Boddie), and *Plodia interpunctella* (Hübner) to several pheromone components and analogs. To quantify the relevant stimulus parameters for the response comparisons, the emission rates of the stimulus delivery system were calibrated for several 12 to 17-carbon pheromone components. The stimulus–response relationships determined for *T. ni*, *H. zea*, and *P. interpunctella* are combined with relationships reported for other insects in the literature, and applications are discussed for the interpretation of pheromone trapping and laboratory bioassays.

Key Words—Pheromone, olfaction, electroantennogram, neurophysiology, *Trichoplusia ni*, *Heliothis zea*, *Plodia interpunctella*, Lepidoptera, Noctuidae, Pyralidae.

INTRODUCTION

The ability of insects to detect odors and to distinguish differences in stimulus levels derives from peripheral and central nervous system (CNS) mechanisms

[1] Postdoctoral fellow employed through a cooperative agreement between the Insect Attractants, Behavior, and Basic Biology Research Laboratory, and the Department of Entomology and Nematology, University of Florida, Gainesville, Florida 32611.

0098-0331/87/0300-0509$05.00/0

that may operate similarly in many animals. Consider, for example, that the rate of action potentials elicited in a peripheral olfactory receptor neuron frequently is found to be graded proportionally to the odorant concentration, irrespective of the insect. This proportionality provides a neurophysiological basis whereby the elicited behavioral responses also can be graded with odorant concentration. (We do not imply that all behavior is graded in this way, because CNS integration and other processes may significantly modify the response.) The concept of the graded behavioral response has been a useful interpretive tool in vertebrate physiology, leading to the development of animal and human psychophysics (Stevens, 1975). Our objective is to quantify and compare several behavioral and neurophysiological stimulus–response relationships and then to demonstrate how the concept of graded response can be applied for interpreting laboratory and field bioassays.

A second focus of this report is to address the problem of pheromone quantification by measuring pheromone emission rates and concentrations.

We analyze the dose–emission rate relationship of a glass-tube odorant dispenser and apply the calibration in quantitative comparisons of neurophysiology and behavior for *Trichoplusia ni* (Hübner), *Heliothis zea* (Boddie), and *Plodia interpunctella* (Hübner).

METHODS AND MATERIALS

Insects and Chemicals

Male *T. ni*, *P. interpunctella*, and *H. zea* pupae were obtained from colonies maintained at this laboratory and held at 70–80% relative humidity, 24–27°C, on a 14:10 light–dark cycle. Adults were 48–72 hr old when tested.

Sex pheromone components of *T. ni*, (*Z*)-7-dodecen-1-ol acetate (*Z*-7:12Ac); *P. interpunctella*, (*Z,E*)-9,12-tetradecadien-1-ol acetate (*Z,E*-9, 12:14Ac); *H. zea*, (*Z*)-11-hexadecenal (*Z*-11:16Al); and *Heliothis virescens* (F.), (*Z*)-9-tetradecenal (*Z*-9:14Al) and tetradecanal (14Al) were provided by Drs. J.H. Tumlinson and K.W. Vick of this laboratory. They were analyzed by gas–liquid chromatography (GLC) either on a 3% OV-1® 1.8-m packed column or 36-m capillary column and found to be >99% pure. The *Z*7:12Ac also was analyzed on a CPS-2 50-m liquid crystal capillary column by R.R. Heath of this laboratory. To calibrate dispenser release rates at low doses, samples of two of the pheromone components, *Z*-7:12Ac and *Z,E*-9,12:14Ac, were tritiated. The tritiated pheromone components were additionally purified by thin-layer chromatography and then by silicic-acid-column chromatography just before use because their lability increased after tritiation. Their specific activities were 0.804 and 0.951 Ci/mmol, respectively, as determined by GLC and liquid scintillation counting (LSC) using external standards.

Dispensers

Two types of pheromone delivery system were used, a glass-tube and a rubber-septa dispenser. The glass-tube dispensers were assemblies of ground-glass joints described in Mayer (1973) and Mayer et al. (1984). The desired quantity of a pheromone component diluted in 0.5 ml of hexane was pipetted into the assembly. The dispenser was rotated under aeration at 200 cm^3/min for 30 sec to coat the inside uniformly and to evaporate the hexane.

The rubber-septa system was one similar to that developed by Heath and Tumlinson (1986). Prior to loading, the 5-mm-ID × 9-mm-long rubber septa (A.H. Thomas Co.) were Soxhlet extracted in methylene chloride for 24 hr and air dried. The Z-7 : 12Ac was applied to the well of a septum in 50-μl aliquots of hexane, and the septum was aired in a hood for two days before use. For testing, the septa were placed in any one of three different delivery assemblies. One was a five-part assembly consisting of a brass Swagelok® 1.587-cm to 0.635-cm reducer, a 1.587-cm to 0.952-cm reducing union, and a 0.952-cm to 0.635-cm reducing port connector, with a 0.635-cm knurled nut at the inlet and a 0.635-cm Teflon® ferrule at the outlet. Another assembly was identical except that the metal was stainless steel. The third delivery system was the glass-tube assembly described above (without an initial pheromone coating).

Prior to pheromone collection or to use in a bioassay, the dispensers were purged for 30 sec with 200 cm^3/min of filtered dry air. The pheromone was delivered by passing filtered dry air through the glass-tube assembly at either 50 or 200 cm^3/min.

Collection and Analysis of Emissions

Three different methods were used in determining the glass-tube dispenser emission rates. Radiolabel analysis of pheromone components collected onto cotton filters was used for emissions at the 50 cm^3/min flow rate. GLC analysis of pheromone components collected in capillaries was used for emissions at 200 cm^3/min with doses between 10 and 1000 μg (0.044–4.4 μmol). The third method used a set of electroantennogram (EAG) bioassays combined with data from the radiolabeled calibration and from a calibration of rubber-septa emission rates by R.R. Heath of this laboratory.

Radiolabeled Pheromone Components. Emission rates of Z-7 : 12Ac and Z,E-9,12 : 14Ac at 50 cm^3/min were determined for doses between 0.08 and 10 μg (3.2×10^{-4}–4×10^{-2} μmol) by LSC analysis of radiolabeled pheromone components collected onto cotton filters. The dispensers were attached with Swagelok connectors to air samplers consisting of 5-mm-ID × 10-cm-long brass tubes stuffed with 35-mg cotton filters at each end. The filtering efficiency of the air samplers ranged from 0.9 to 0.97 as determined by comparing the radioactivity collected on the front and back filters. After the tritiated com-

pounds were collected, the filters were combusted in a Packard model 306® sample oxidizer. The oxidizer distilled the resultant tritiated water vapor into 10 ml of Packard Monophase-40® scintillation fluid cocktail. The efficiency of the oxidizer was monitored by external standards that indicated a negligible loss of radioactivity in this stage of the analysis. (Some of the emissions were collected independently by the capillary trap method described below, in which case the collected pheromone was rinsed with hexane directly into the scintillation cocktail.) The radioactivity of the cocktails was counted for 1 hr in a Packard model 2450® liquid scintillation counter calibrated by external standards.

GLC Analysis of Emissions of Unlabeled Pheromone Components at 200 cm^3/min. For pheromone component doses of 10–1000 μg (0.044–4.4 μmol), the collection device used was that described by Brownlee and Silverstein (1968). The emissions were collected in glass or stainless-steel capillaries connected to the dispenser by glass or Swagelok adaptors. The capillary was inserted into a metal tube heated at the dispenser end and chilled with acetone and Dry Ice at the outlet end. After a 3-min collection interval, the capillary was rinsed with 300 μl of hexane or diethyl ether into a calibrated centrifuge tube. In one series of tests the capillary effluent was passed through 3 ml of hexane to determine the collection efficiency of the capillary (about 80%). In another series of tests emissions from 100-μg doses of *Z*-7 : 12Ac were collected for 15-sec increments from 15- to 180-sec periods to determine a regression of quantity released on time.

The centrifuge tube contents were reduced for quantitative analysis by evaporation under dry nitrogen to remove excess hexane. Evaporative loss was calibrated in several cases by external standards using related compounds of similar volatilities but different GLC retention times. Aliquots from the centrifuge tubes were analyzed on a Varian model 210 GLC system with a flame ionization detector. The 1.8-m × 2-mm-ID glass column was packed with 3% OV-1 on 100–120 mesh Gas-Chrom-Q®, and the flow of nitrogen carrier was 30 cm^3/min. All analyses were isothermal, with the injector and detector at 200°C and the oven at 130–150°C. A Spectra-Physics model 4100 computing integrator was used for recording and quantitating the amounts recovered.

EAG Analysis of Z-7: 12Ac Emission at 200 cm^3/min. The glass-tube dispenser emission rates at the 200 cm^3/min flow rate for doses of *Z*-7 : 12Ac between 0.1 and 10 μg (4.4×10^{-4}–4.4×10^{-2} μmol) were estimated by performing a set of three separate EAG bioassays on *T. ni* males. Two of the bioassays were done to determine a regression of EAG on concentration. In the third bioassay, EAGs performed at 200 cm^3/min were correlated with the concentrations predicted from the regression. The expected emission rate from a given dose then was determined by multiplying the predicted concentration by the total air flow in the plume passing over the antenna.

The first bioassay was done primarily at the 50 cm^3/min flow rate using the glass-tube dispenser. Here, the Z-7 : 12Ac concentrations delivered to the antenna were calculated from the radiolabeled pheromone calibration. The GLC measurements described above, calibrating Z-7 : 12Ac emission rates from the glass-tube dispenser at doses of 10, 31.6 and 100 μg, were used with EAGs of these three doses at the 200 cm^3/min flow rate.

The second EAG bioassay was done using a rubber-septa formulation, calibrated by R.R. Heath of this laboratory. The emission rates were estimated by interpolating between two curves of emission rate against dose, one at a 250 cm^3/min rate of flow through the brass assembly, and one at 100 cm^3/min.

The equation chosen to regress the EAG response magnitude against concentration was a power function (see, e.g., Mayer and Mankin, 1985) of the form:

$$\log(R) = A + B \log(C) \tag{1}$$

where R is the EAG response in $-$mV, A and B are regression constants, and C is the pheromone concentration in μmol/cm^3. This equation was applied to the uncalibrated, low-dose EAG responses at 200 cm^3/min to estimate what concentrations had been present at the antenna when the responses were elicited. Finally, the release rates were calculated by multiplying the predicted concentration at each dose by the total flow rate.

Bioassays

Neurophysiological. Electroantennogram responses of *T. ni* and *H. zea* to Z-7 : 12Ac and Z-11 : 16Al, respectively, were measured by procedures similar to those described in Mayer et al. (1984). The concentrations delivered to the antennae for the *T. ni* EAGs were estimated from the 50 cm^3/min emission rate calibration and the rubber-septa calibration described above. The concentrations delivered in the *H. zea* bioassay were determined from the 200 cm^3/min emission rate calibration for doses of Z-11 : 16Al above 3 μg. The concentrations for lower doses were estimated by extrapolating from the curve for higher doses and using the same slope as for the Z-7 : 12Ac emission rates, as described in the Results section.

Single-sensillum recordings from *T. ni*, and *H. zea* were obtained as in Mayer (1968) using electrodes made from tungsten wire, sharpened electrolytically to less than a 1-μm tip diameter. Adult males were secured with wax, and the recording electrode was placed at the base of the sensillum. Signals were amplified and filtered (bandpass 1–10 kHz) with a Grass P15 AC preamplifier. The signals were monitored with a Tektronix 5113 dual-beam storage oscilloscope. Analysis and storage of data were performed on a Digital Equipment Corporation MINC Declab-23® microcomputer by a procedure similar to that described in O'Connell et al. (1973).

Flight Tunnel. The flight-tunnel bioassays for *T. ni* and *P. interpunctella* are reanalyses of data from two earlier reports by Mayer (1973) and Mankin et al. (1980). In those reports the concentration of pheromone in the tunnel had been estimated by dividing the dispenser output by the total tunnel airflow. However, this estimate of concentration is correct only if complete mixing of pheromone with air occurs. Results from subsequent flight and EAG bioassays had suggested that complete mixing was not occurring, even though $TiCl_4$ smoke released from the dispenser into the tunnel appeared to be well-mixed when the smoke reached the downwind end.

To avoid relying on visual estimates of the completeness of mixing in the tunnel, we determined the downwind pheromone concentration at the insect release point by an EAG bioassay. Electroantennograms were recorded from 10 *T. ni* males in the tunnel with the stimulus airflow through the dispensers set to 50 cm^3/min. Each male was tested with Z-7 : 12Ac at doses of 3.16, 10, and 31.6 μg (0.014–0.14 μmol). The upwind concentration at the dispenser release point was calculated by dividing the emission rate by the dispenser flow rate. The downwind concentration to which each male had been exposed was calculated from the regression of EAG on concentration described in the previous section. To estimate the mean dilution factor, the upwind concentration was divided by the downwind concentration. The mean dilution factor determined from the three different doses in the EAG bioassay then was applied to all dispenser doses to determine the concentrations in the tunnel.

RESULTS

Although the dispensers were calibrated primarily to relate responses from the behavioral bioassays to responses from the neurophysiological bioassays, the calibrations are interesting in themselves and will be described first. The calibrations then are compared with those of other types of dispensers, and the most significant features of the release pattern are generalized to other release systems.

Two of the findings in this section warrant particular emphasis. First, the emission rate of pheromone from the glass-tube dispenser (and probably from many other types of dispenser as well) is not linearly proportional to dose. The greatest deviations from linearity occurred at the upper and lower ends of the dosage range. Such deviations lead to overestimation of stimulus levels at both high and low doses of pheromone. This can lead to errors of interpretation when a dose–response bioassay is not referenced to the concentration in the airstream. Second, the plume of pheromone in a wind tunnel remains relatively undiluted under most conditions. Measurements by EAG indicate that the mean dilution factor may be no larger than 10–20, even when a visual indicator, e.g., a smoke plume, appears well dispersed. The instantaneous dilution factor varied consid-

erably about the mean in a pattern intermediate to the EAG pattern described for the point source and the continuous cloud source by Baker et al. (1985).

Glass-Tube Dispenser Emission Rates. The relationship between dose and emission rate for the glass-tube dispenser was similar for all of the pheromone components tested at both 50 and 200 cm^3/min flow rates and appeared to follow a general pattern predicted by current theories of molecule-surface dynamics (see Tully and Cardillo 1984). At doses from $1 \times 10^{-3.5}$–1×10^{-1} μmol, the emission rate increased with increasing dose. Above this range the emission rates reached a constant level, independent of dose. Thus we found it necessary to divide the calibration curves for each chemical into multiple segments. The regression equations of best fit for doses of less than 100 μg are listed in Table 1, and the data are shown in Figures 1 and 2.

The inset in Figure 2 shows the Z-7 : 12Ac emission rates calculated for the EAG calibration at 200 cm^3/min for doses below 10 μg. The segment of the Z-7 : 12Ac line labeled GC is redrawn from the GLC calibration on the main graph, and the segment labeled EAG is the part calibrated by EAG. In the EAG segment, the emission rates are calculated from the concentrations predicted at different EAG levels by the *T. ni* EAG–concentration regression line, TNE, in Figure 3. The top part of the dotted curve in the inset of Figure 2, labeled Z-11 : 16Al, also is redrawn from the main graph. The extension of this curve, the segment with larger dots, is an assumption that the curve for Z-11 : 16Al is parallel to the curve for Z-7 : 12Ac. The Z-11 : 16Al emission rate curve was used to estimate the concentrations for the regression of *H. zea* EAG on concentration, HZE, in Figure 3.

The amounts of Z-7 : 12Ac release over 15-sec periods from 15 to 180 sec yielded a statistically linear regression over the 3-min period (Table 2). (Note: theoretically, the release rate decreases exponentially, but most of the decrease occurs during the initial 30-sec purge.)

Comparison of Glass Tube with Other Dispensers. Because pheromones are not usually dispensed from glass, it is worthwhile to compare the glass tubes with other substrates and to generalize some of the findings, if possible. The (initial) rate of emission of pheromone from the glass tube is higher than from most slow-release formulations. For example, the half-life of Z-7 : 12Ac on rubber septa is 34.8–35.9 days (Butler and McDonough, 1979). Based on this half-life, the initial emission rate from a septum dosed with 1 mg is 6.1×10^{-5} μmol/min. The same initial emission rate of Z-7 : 12Ac from the glass tube is achieved by a dose of 3.98×10^{-3} μmol (890 ng), according to the inset in Figure 2. This also can be compared with the measurement by Baker et al. (1981) of a 1.62×10^{-5} μmol/min emission rate from a septum dosed with 1 mg of Z-8 : 12Ac.

Comparisons of Z,E-9,12 : 14Ac released from different substrates reveal a pattern similar to that shown by Z-7 : 12Ac. A polyethylene cap loaded with 33.7 μmol (8.5 mg) of Z,E-9,12 : 14Ac emits at the rate of 3.10×10^{-5} μmol/

TABLE 1. REGRESSION EQUATIONS FOR RELEASE RATES OF SEX PHEROMONES AND RELATED CHEMICALS AT DOSES BELOW 100 μg[a]

Chemical	Flow rate (cm^3/min)	Regression constant	Estimate	Standard error of estimate	F	R^2
Z-1,12:17	200	A	−0.72	0.35	43.24[b]	0.73
		B	1.51	0.23		
Z-11:16Al	200	A	−2.01	0.21	65.11[b]	0.80
		B	1.38	0.17		
14Al	200	A	−1.29	0.34	19.51[b]	0.55
		B	1.63	0.37		
Z-9:14Al	200	A	−1.35	0.18	55.33[b]	0.58
		B	1.34	0.18		
Z-9:14For	200	A	−1.95	0.17	94.30[b]	0.78
		B	1.18	0.12		
Z,E-9,12:14Ac	50	A	−3.94	0.68	17.82[c]	0.78
		B	1.09	0.26		
Z-7:12Ac	50	A	−1.30	0.42	80.46[b]	0.82
		B	1.80	0.20		
Z-7:12Ac (by GLC)	200	A	−1.12	0.04	1057.03[b]	0.87
		B	1.37	0.04		
Z-7:12Ac (by EAG)[d]	200	A	0.30	0.44	186.72[b]	0.80
		B	2.05	0.15		

[a] The regression equations have the form: log(emission rate) = $A + B$ log(dose), where A and B are regression constants in the table, the units of emission rate are μmol/min, and the units of dose are μmol.
[b] Statistically significant at the 0.001 probability level.
[c] Statistically significant at the 0.01 probability level.
[d] See inset in Figure 2.

min (Mankin et al., 1980), which compares with a glass tube loaded with 0.18 μmol (45 μg) (Figure 1). A Fiberglas®-coated screen dosed with 0.397 μmol (0.1 mg) of *Z,E*-9,12 : 14Ac emits 1.33×10^{-6} μmol/min (Mankin et al., 1983), which is slightly less than the emission rate from the glass-tube dispenser.

More important for general comparison, the theory of molecule–surface dynamics (e.g., Tully and Cardillo, 1984) predicts that the emission of pheromone from any dispenser, except an ideal inert matrix, follows a pattern similar to that found for the glass tubes. At some point near the upper end of the dosage range of behavioral relevance, the low vapor pressure of pheromone limits the rate of pheromone release. At low doses the pheromone remains adsorbed to low-energy sites on the substrate. The actual doses where such effects occur

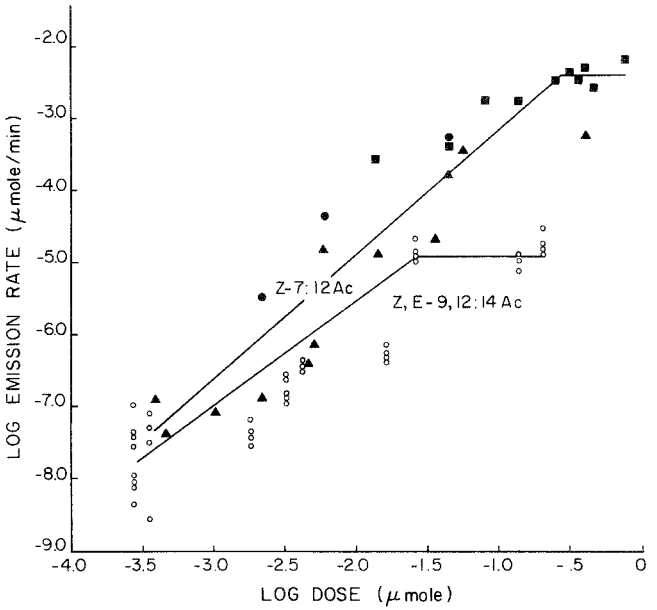

FIG. 1. Release rates of Z-7 : 12Ac and Z,E-9,12 : 14Ac from glass dispensers at a flow rate of 50 cm^3/min: Triangles, means of four to seven replications with ^{3}H-labeled Z-7 : 12Ac collected by the air sampler; closed circles, mean of four replications with ^{3}H-labeled Z-7 : 12Ac collected by cold trap; squares, means of 8–19 replications with unlabeled Z-7 : 12Ac collected by cold trap; open circles, single measurements with ^{3}H-labeled Z,E-9,12 : 14Ac collected by the air sampler.

depend on the substrate, the molecular weight, and the functional groups of the pheromone molecule.

Neurophysiological Bioassays. In the single-neuron study, the responses of pheromone-sensitive receptor neurons in *T. ni* occurred at concentrations only above $1 \times 10^{-4.6}$ μmol/cm^3, which is about the same as the EAG threshold. Similarly, pheromone-sensitive neurons in the long, sexually dimorphic sensilla spaced in rows on the proximal 40–50 subsegments of the male *H. zea* antennae responded to doses of Z-11 : 16Al above about $1 \times 10^{-3.4}$ μmol (0.1 μg). The emission rate of Z-11 : 16Al was not calibrated at this level; however, by extrapolation from the inset of Figure 2, this dose appears to correspond to an emission rate of about 1×10^{-8} μmol/min, and a concentration at the antenna of about $1 \times 10^{-11.1}$ μmol/cm^3 (Figure 3). The *H. zea* and *T. ni* receptor neurons, which are sensitive to their major pheromone components thus appear to have similar sensitivities, and the similarity of the two EAG response curves is in agreement with this finding (Figures 3–5).

The EAG responses of *T. ni* and *H. zea* to Z-7 : 12Ac and Z-11 : 16Al,

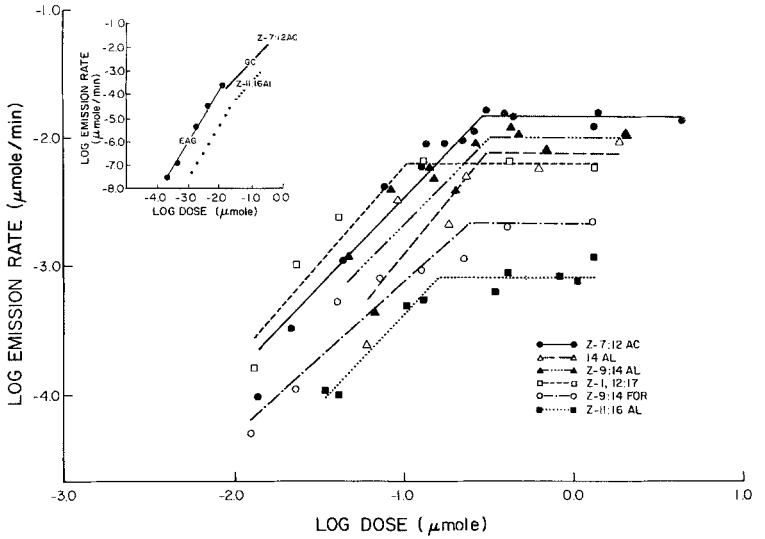

FIG. 2. Release rates of pheromone components from glass dispensers at a flow rate of 200 cm^3/min. All collections were by cold trap and analyses were by GLC. Closed circles, Z-7:12Ac; open triangle, Z-9:14Al; closed triangle, 14Al; open circle, Z-9:14For; closed square, Z-11:16Al; open square, Z-1,12:heptadecadiene. Inset shows EAG calibration of release rates of Z-7:12Ac for doses below 10 μg and the extrapolation of the emission rate of Z-11:16Al for doses below 10 μg.

respectively, are shown in Figure 3. No significant differences in the *T. ni* EAG response were noted in tests with the three different rubber-septa assemblies (brass, stainless steel, or glass). We note also that the *T. ni* EAG levels are somewhat lower than those given in Mayer et al. (1984) because improvements in the mixing chamber of the stimulus delivery system lowered the peak concentrations delivered to the antenna. The regression of *T. ni* EAG response on concentration was used to calculate the emission rate curve in the inset of Figure 2 that estimates emission rates of low doses of Z-7:12Ac at the 200 cm^3/min flow rate. The *T. ni* regression also was used to determine the dilution factor in Table 3 for the wind-tunnel bioassays in Figure 4. The regression equations are listed in Tables 4 and 5.

Wind Tunnel Bioassays. The dilution ratios measured by the wind-tunnel EAGs show that, contrary to earlier assumptions, there was not enough turbulence to cause complete mixing of pheromone in the bioassays of anemotaxis in *T. ni* (Mayer, 1973) and *P. interpunctella* (Mankin et al., 1980). The mean dilution ratio was 23.7 (Table 3). If the Z-7:12Ac plume in the EAG tests had mixed completely with the tunnel air, the mean dilution ratio would have been 51,200, three orders of magnitude higher than the EAG-derived ratio. Conse-

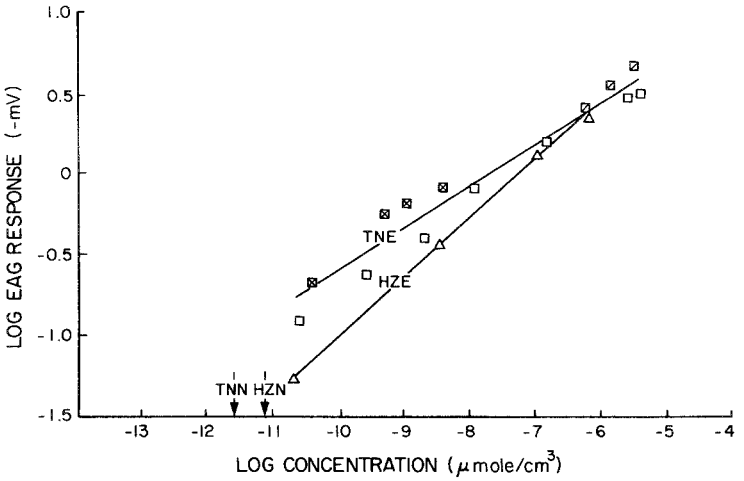

FIG. 3. Concentration–response relationships for *T. ni* and *H. zea* neurophysiological bioassays. TNE: regression of *T. ni* EAG response on Z7–12 : Ac concentration; open squares are means of 10 replications with glass-tube dispenser at 50 cm^3/min flow rate, squares with slash are means of 10 replications with glass-tube dispenser at 200 cm^3/min flow rate, squares with cross are means of 30 replications with rubber septa at 200 cm^3/min flow rate. HZE: regression of *H. zea* EAG response on Z-11 : 16Al concentration; triangles are means of 13 replications with glass-tube dispenser at 200 cm^3/min flow rate. TNN: lowest concentration eliciting detectable response by *T. ni* pheromone receptor neurons sensitive to Z-7 : 12Ac. HZN: lowest concentration eliciting detectable response by *H. zea* pheromone receptor neurons sensitive to Z-11 : 16Al. Regression equations are listed in Table 4.

TABLE 2. REGRESSION EQUATIONS FOR RELEASE RATES FROM DISPENSERS[a]

Flow rate (cm^3/min)	Regression coefficient ($\times 10^{-5}$)	Standard error of estimate ($\times 10^{-5}$)	F	R^2
50	1.10	.08	211.54[b]	0.99
100	3.86	.30	168.29[b]	0.99
200	9.67	.89	119.18[b]	0.98

[a] Dosed with 0.44 μmol (100 μg) Z-7:12Ac at flow rates of 50, 100, and 200 cm^3/min. The regression equations have the form: emission = $K \times$ time, where K is the regression coefficient, emission is given in μmol and time is in seconds.

[b] Statistically significant at the 0.01 probability level.

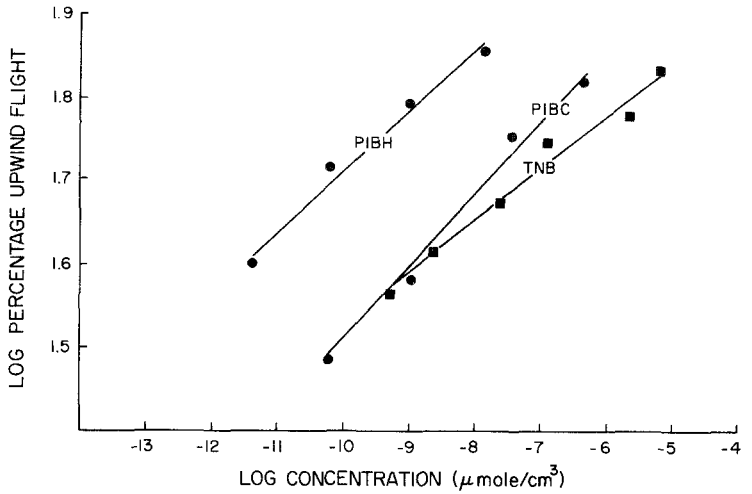

FIG. 4. Concentration–response relationships for wind-tunnel bioassays. The regression equations are given in Table 4. TNB line with squares, anemotactic response to *Z*-7 : 12Ac by *T. ni*; PIBC line with circles, anemotactic response to *Z,E*-9,12 : 14Ac by *P. interpunctella* at 23°C.; PIBH line with circles, anemotactic response to *Z,E*-9,12 : 14Ac by *P. interpunctella* at 34°C.

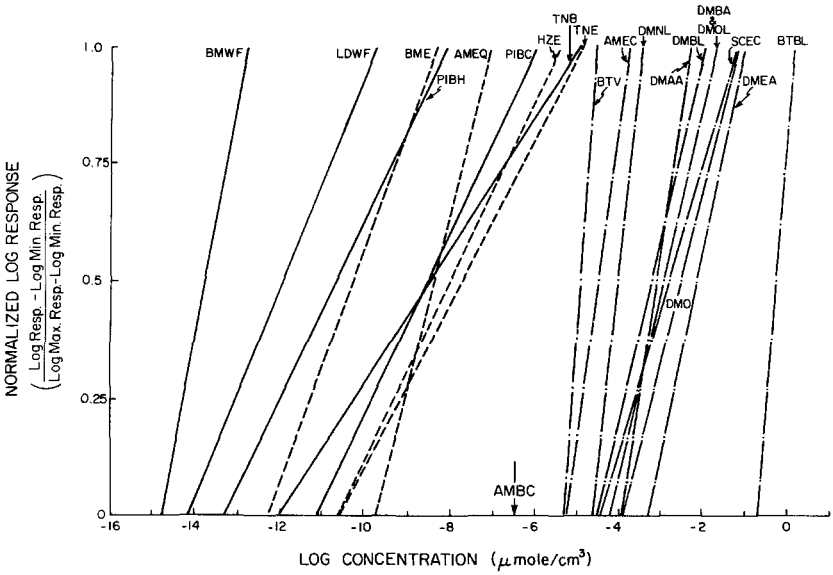

FIG. 5. Comparison of normalized behavioral and neurophysiological responses of several insect species to various odorants. Solid lines indicate behavioral response. Dashed lines indicate EAGs in response to a sex pheromone component. Dot-dashed lines indicate EAGs in response to a non-pheromonal odorant. AMBC is the behavioral threshold of female *A. mellifera* to caproic acid. See Table 5 for key to abbreviations.

TABLE 3. EAG BIOASSAY OF Z-7:12Ac DILUTION RATIO IN WIND TUNNEL[a]

Dispenser dose (μg)	log EAG response (−mV)	Log concentration (μmol/cm^3) At dispenser outlet	Log concentration (μmol/cm^3) At end of tunnel	Dilution ratio
3.16	−0.056	−6.70	−8.0	20.0
10.0	0.223	−5.95	−7.0	11.2
31.6	0.422	−4.50	−6.1	39.8

[a] The concentration at the end of the tunnel was estimated from Figure 3. The concentration at the dispenser outlet was estimated from the release rates in Figure 1, with the release rate divided by 50 cm^3/min to calculate concentration.

quently, we have revised upward the estimates of pheromone concentration in the two bioassays and recalculated the stimulus–response regression equations.

The pheromone concentration in the wind tunnel was recalculated from the new emission rate curves listed in Table 1 and the mean wind-tunnel dilution factor in Table 3. The regression constants of Eq. 1, based on the revised concentrations, are listed in Table 4, and the new concentration–response regressions are shown in Figure 4. The new estimates indicate that 50% upwind anemotaxis was elicited in *T. ni* at concentrations above about 1×10^{-7} μmol/cm^3 of Z-7:12Ac. Extrapolating the curve to the 25% level, at log percentage upwind flight = 1.4, we find that the threshold occurs near 1×10^{-12} μmol/cm^3. The range of anemotactic response by *P. interpunctella* at 23°C was similar to that for *T. ni*. At 34°C (PIBH), the magnitude of response of *P. interpunctella* was higher than at 23°C (PIBC), but the slopes of the two curves were statistically indistinguishable.

DISCUSSION

The remainder of this report applies a quantitative perspective to problems of behavioral and neurophysiological response. We begin with some comparisons of pheromone emission rates from glass-tube dispensers and natural emitters, and apply the dispenser calibrations to interpretations of behavioral responses in a wind tunnel. Then we discuss how sensation magnitude theory combines the results of this and a number of other studies in the literature into a common framework.

One additional point must be addressed briefly, i.e., the choice of odorant concentration as the common parameter for interrelating the behavioral and neurophysiological responses. It has been noted elsewhere (Elkinton and Cardé,

TABLE 4. REGRESSION EQUATIONS FOR BEHAVIORAL AND EAG RESPONSES OF INSECTS TO BEHAVIORALLY ACTIVE CHEMICALS[a]

Insect	Bioassay key	Regression constant	Estimate	Standard error of estimate	F	R^2
A. mell. male	AMEC	A	2.38	0.001	9999.9	0.99
		B	0.38	0.0003		
A. mell. male	AMEQ	A	4.46	0.002	9999.9	0.99
		B	0.47	0.0002		
B. terr. female	BTBL	A	−0.30	0.01	13265.3	0.99
		B	1.66	0.01		
B. terr. female	BTV	A	2.63	0.21	219.5	0.99
		B	0.64	0.04		
B. mori male	BMWF	A	6.64	0.67	53.9	0.95
		B	0.36	0.05		
B. mori male	BME	A	1.91	0.17	126.8	0.98
		B	0.19	0.02		
D. mela. female	DMAA	A	1.35	0.11	210.5	0.99
		B	0.52	0.04		
D. mela. female	DMBA	A	1.01	0.04	747.7	0.99
		B	0.40	0.01		
D. mela. female	DMBL	A	1.29	0.09	256.1	0.99
		B	0.46	0.03		
D. mela. female	DMEA	A	0.86	0.04	710.9	0.99
		B	0.55	0.02		
D. mela. female	DMNL	A	2.59	0.23	132.7	0.99
		B	0.63	0.05		
D. mela. female	DMO	A	0.20	0.06	289.3	0.98
		B	0.36	0.02		
D. mela. female	DMOL	A	1.58	0.09	144.6	0.95
		B	0.36	0.03		
H. zea male	HZE	A	2.90	0.21	238.4	0.83
		B	0.39	0.03		
L. dispar male	LDWF	A	4.31	0.50	29.2	0.88
		B	0.18	0.03		
P. inter. male	PIBC	A	2.37	0.05	191.3	0.99
		B	0.09	0.006		
P. inter. male	PIBH	A	2.51	0.07	120.1	0.98
		B	0.08	0.007		
Sc. scol. female	SCEC	A	2.61	0.0005	9999.9	1.00
		B	0.54	0.0002		

TABLE 4. Continued

Insect	Bioassay key	Regression constant	Estimate	Standard error of estimate	F	R^2
T. ni male	TNB	A	2.16	0.05	95.1	0.96
		B	0.06	0.006		
T. ni male	TNE	A	2.01	0.06	1443.7	0.86
		B	0.26	0.007		

[a]The regression equations have the form: log(response) = A + B log(concentration), where A and B are regression constants in the table. The concentration is specified in μmol/cm^3. Details of the response measures and references are specified in the bioassay keys in Table 5.

1984; Mankin and Mayer, 1983a) that an odor receptor neuron reacts to the rate of adsorption of odorant onto its receptor sites rather than to the odorant concentration. The rate of adsorption, however, is directly proportional to the concentration because the final approach of odorant molecules to the antenna is controlled by molecular diffusion over a thin boundary layer. The rate of adsorption (μmol/sec) is equal to the overall flux [μmol/(cm^2 sec)] times the collecting surface area for the receptor site (cm^2), which is the sensillum surface. The flux in turn is equal to the concentration (μmol/cm^3) times a parameter called the deposition velocity, which for pheromonal molecular diffusion is about 1 cm/sec (Mankin and Mayer, 1984). Because the receptor surface area and the deposition velocity vary negligibly relative to the concentration, it is convenient to use the more familiar parameter of concentration as the unit of stimulation.

Comparisons between Pheromone Emission Rates of Glass-Tube Dispensers and Natural Emitters. The evaporation of pheromone from a relatively inert surface like glass or from a pheromone gland both occur by similar physical processes; consequently, any differences in the range of release rates between glass dispensers and natural emitters is due primarily to differences in the exposed surface area. There are examples in the literature where the emission rate of pheromone from a female insect is comparable to the maximal emission from a glass-tube dispenser. The emission rate of Z-7 : 12Ac from *T. ni* virgin females has been measured at 3.1×10^{-5} μmol/min by Sower et al. (1971), 5.3×10^{-5}–9.7×10^{-5} μmol/min by Björstad et al. (1980), and 1.06×10^{-5} μmol/min by Baker et al. (1981). These rates are about an order of magnitude less than the maximum rates for the glass dispensers in Figures 1 and 2.

Another example where the maximal emission rate from a glass tube and from a female are likely to be similar is the measurement of the emission rate of (+)-*cis*-7,8-epoxy-2-methyloctadecane from *Lymantria dispar* L. females. Charlton and Cardé (1982) reported that the maximal emission rate from a virgin female was 3.8×10^{-3} μmol/min and the mean rate was 1.2×10^{-3} μmol/min. In contrast the pheromone emission rate from *P. interpunctella* females,

TABLE 5. LIST OF KEYS TO CURVES IN FIGURE 4 AND REGRESSION EQUATIONS IN TABLE 4.

Key	Reference	Chemical	Response Measure
AMBC	Schwarz (1955)	Caproic acid	50% Behavioral response
AMEC	Kaissling (1971)	Caproic acid	EAG (−mV)
AMEQ	Kaissling (1971)	*E*-2, oxo-9:10OOH	EAG (−mV)
BME	Kaissling (1971)	*E,Z*-10,12:16OH	EAG (−mV) from Figure 42
BMWF	Kaissling (1971)	*E,Z*-10,12:16OH	% Wing flutter
BTBL	Fonta and Masson (1984)	Butanol	EAG (−mV)
BTV	Fonta and Masson (1984)	Vanillin	EAG (−mV)
DMAA	Venard and Pichon (1984)	Amyl acetate	EAG (−mV)
DMBA	Venard and Pichon (1984)	Butyl acetate	EAG (−mV)
DMBL	Venard and Pichon (1984)	Butanol	EAG (−mV)
DMEA	Venard and Pichon (1984)	Ethyl acetate	EAG (−mV)
DMNL	Borst (1984)	3-Nonanol	EAG (−mV)
DMO	Venard and Pichon (1981)	Octane	EAG (% of butanol standard)
DMOL	Borst (1984)	3-Octanol	EAG (−mV)
HZE	This report	*Z*-11:16Al	EAG (−mV)
LDWF	Elkinton et al. (1984)	(+)-Disparlure	% Wing flutter
PIBC	Mankin et al. (1980)	*Z,E*-9,12:14Ac	% Upwind flight at 23°C
PIBH	Mankin et al. (1980)	*Z,E*-9,12:14Ac	% Upwind flight at 34°C
SCEC	Wadhams (1982)	α-Cubebene	EAG [% of (+)-*threo*-4-methyl-3-heptanol standard]
TNB	Mayer (1973)	*Z*-7:12Ac	% Upwind flight at 22°C
TNE	Mayer et al. (1984) and this report	*Z*-7:12Ac	EAG (−mV)

1.95×10^{-7} μmol/min (Sower and Fish, 1975), falls near the lower limit of the dispenser release rate calibration in Figure 1 at $10^{-6.7}$ μmol/min.

General Comparisons of Pheromone Concentrations in Plumes Emitted by Dispensers and in Plumes from Natural Emitters. It is somewhat misleading to compare the dispensers with the females solely on the basis of emission rate. Typically, the emitting surface of the dispenser is greater than the area of the pheromone gland, so the dispenser can have a higher overall emission rate than the gland. But the pheromone concentrations in the emitted plumes of the dispenser and the female cannot exceed a limit imposed by the saturated vapor concentration. This concentration limit is often at the upper levels of emission rates of either pheromone glands or pheromone dispensers.

Consider, for example, the case of a hemispherical pheromone gland with a radius between $r = 0.03$ and $r = 0.3$ cm. The maximum physically possible release rate, *ER*, can be estimated from the equation (Hirooka and Suwanai, 1976):

$$ER = 2\pi rDC_v \tag{2}$$

where D is the diffusion coefficient (about 0.04 cm^2/sec), and C_v is the saturated vapor concentration. Values for C_v can be estimated from the literature. Hirooka and Suwanai (1976) list saturated concentrations of 7.0×10^{-5} μmol/cm^3 for 12Ac and 2.8×10^{-5} μmol/cm^3 for 14Ac. Olsson et al. (1983) found the saturated vapor pressure for Z-7 : 12Ac to be 0.562 *Pa*. This can be converted to saturated vapor concentration by applying the Ideal Gas Law, $PV = nRT$: for 1 *Pa* = 0.987×10^{-5} atm, 1 atm = 1.01×10^5 newton/m^2, and $R = 8.31$ newton m/°K/mol, the saturated vapor concentration at $T = 290$°K (= 20°C) is 2.30×10^{-4} μmol/cm^3 ($1 \times 10^{-3.64}$ μmol/cm^3). For 12Ac with $r =$ 0.3 cm, this release rate is about $1 \times 10^{-3.0}$ to $1 \times 10^{-3.5}$ μmol/min, and for 14Ac with $r = 0.03$ cm, it is about $1 \times 10^{-4.9}$ μmol/min. The maximum possible release rate for *T. ni* females is near the measured release rate. Based on the above, we conclude that *T. ni*, but not *P. interpunctella*, females release sex pheromone at nearly the highest possible rate.

As with the female *T. ni*, the concentration of Z-7 : 12Ac in the plume from the glass dispensers approaches but does not completely reach saturation. When the release rate is $1 \times 10^{-2.0}$ μmol/min (about the upper limit in Figure 2), the concentration of Z-7 : 12Ac in the dispenser plume is 5×10^{-5} μmol/cm^3 at a dispenser flow rate of 200 cm^3/min, an order of magnitude less than the saturated vapor concentration of about 2.3×10^{-4} μmol/cm^3. The release rates of pheromone from *T. ni* and *L. dispar* females, and from the dispenser, are limited physically as the concentrations approach the saturation vapor concentration.

We expect that similar physical limitations occur for any dispenser operating at physiological temperatures. Thus, when the moth emits pheromone at its highest possible rate, the concentration in its emitted plume will be about

the same as in the plume from the most efficient artificial dispenser. The dispenser can release more pheromone into a larger volume, e.g., by increasing either the surface area or the air flow through the dispenser, but the concentration can be no higher than saturation. It is thus no surprise that calling insects often compete well with field traps.

Comparison of Anemotactic and EAG Response in a Wind Tunnel. The utility of combining dispenser calibration data with stimulus–response data for EAG and behavioral bioassays into a common interpretive framework is illustrated by a reexamination of the anemotactic flight bioassays of *T. ni* and *P. interpunctella* in Mayer (1973) and Mankin et al. (1980). In the original reports, data were presented for pheromone doses up to about 1 μmol (100 μg). This dosage is above the transition point where the emission rate from the dispenser becomes independent of dose (Figure 2). In these assays, the response to increasing doses had seemed anomalous because, in contrast with lower doses, the percentage of upwind flight to the pheromone source failed to increase with dose. On the assumption that the emission rate was proportional to dose, it was hypothesized that a qualitative change in the behavioral response had occurred, i.e., that the moths were induced to switch to a more intensive search pattern in the presence of high pheromone concentrations. Similar hypotheses have been proposed to explain reductions in pheromone trap captures at high pheromone concentrations (e.g., Helland et al., 1985).

Although the original hypothesis indeed may still be valid, the calibration results in this report suggest an alternate explanation for the stimulus–response curves in the *T. ni* and *P. interpunctella* bioassays. Both the behavioral and EAG responses level off when the dose is increased above a critical level. The apparent anomaly disappears when either measure of response is referenced to the actual pheromone concentrations.

General Comparisons of Behavioral and Neurophysiological Responses. To proceed into a more general discussion of interrelationships between insect behavioral and neurophysiological responses requires an assumption that usually has been applied only to vertebrates. The assumption is that a graded olfactory input leads to the production of a graded "sensation" in the CNS that mediates a graded output or behavioral response.

The idea of sensation has considerable importance for the interpretation of insect behavioral and neurophysiological responses because it can be used to generate a number of testable hypotheses. One hypothesis in particular, proposed by Stevens (1975), has been validated many times in vertebrate physiology. Stevens proposed that the magnitude of sensation, and consequently of behavioral response, is a power function of the stimulus intensity. One form of the power function is Eq. 1, which also can be expressed as (Mankin and Mayer, 1983b):

$$R = R_0(C - T)^b \tag{3}$$

where R is the chosen measure of response intensity, R_0, T, and b are regression constants, and C is the odorant concentration. The regression constant, T is analogous to a response threshold, and b is analogous to the conversion factor of an electrical transducer. The parameters T and b are of particular interest in comparisons across bioassays because they are independent of the method of measuring the response, and they may provide a measure of the transduction and central processes that result in behavior.

The power function relationship appears to be valid for all of the insect neurophysiological and behavioral stimulus–response relationships that we have measured or found in the literature, as can be seen in Figure 5. Because a number of different responses were examined, each with a different scale, we transformed the different responses in Figure 5 into a common vertical scale. The transformation procedure makes use of the fact that the concentration, C, and the exponent, b, in the power function (Eq. 3) are independent of the response measure. This permits the different responses to be compared on an equal basis by using a normalizing function (cf. Mankin et al., 1980):

$$\text{normalized log resp.} = \frac{\text{log resp.} - \text{min. log resp.}}{\text{max. log resp.} - \text{min. log resp.}} \tag{4}$$

It should be noted that stimulation must be given over the full range from zero to maximal response to obtain the denominator in Eq. 4. Otherwise the range will be truncated. The regression constants of the stimulus–response relationships in Figure 5 are shown in Table 4.

There are two patterns that appear upon inspection of Figure 5. One is that neurophysiological responses occur at concentrations no more than about two orders of magnitude above the behavioral responses. The second is that responses to the most behaviorally significant pheromone components and responses to other odors, such as host-plant compounds, fall into two distinct groups. Behavioral, EAG, and single-unit responses to sex pheromone components are in the range 1×10^{-9}–1×10^{-15} μmol/cm^3. Responses of EAGs to other chemicals are four or more orders of magnitude less sensitive. An estimate of the threshold can be obtained from the points where the regressions cross the axis. This is the point of 25% response (log = 1.4).

Interpretation of Relationships among Behavioral and Neurophysiological Responses. The two patterns of consistent relationships between behavioral and neurophysiological responses in Figures 3 and 4 may reflect some underlying similarities in the way these different insect olfactory systems operate. A simple model of the olfactory process can be constructed to explain these relationships from concepts of sensation and signal detection theory. The details of such a model are presented in Mankin and Mayer (1983a), Mayer et al. (1984), and Mayer and Mankin (1985).

In brief, the model comprises: (1) a number of detectors that individually

respond at a level that is a power function of the stimulus intensity; (2) a central processor that linearly sums the individual responses to give a sensation; and (3) a behavioral output that is proportional to the intensity of sensation. The summing at a hypothetical central processor explains how a behavioral response can be measured at stimulus levels where a corresponding response cannot be measured at a single receptor neuron, i.e., why the behavioral response can be detected at concentrations up to two orders of magnitude below the single-unit response. This idea is supported by experimental evidence that the pheromone receptor neurons converge into a macroglomerulus from which interneurons emerge that respond to peripheral stimulation at levels below what can be detected in single-unit recordings (Boeckh and Boeckh, 1979).

The EAG fits into the model as a correlative of the summed input to the central processor. The EAG is presumed to be a bulk measure of the summed generator potentials that drive the action potential responses of the receptor neurons; consequently, the EAG is predicted to be a power function of the stimulus intensity (Mayer et al., 1984).

If there were no uncertainties in the detection of the odorant or in the behavioral and neurophysiological measures of the response, the different behavioral and neurophysiological response curves for each insect in Figure 5 would merge; i.e., they would simply be different but equivalent measures of the hypothetical curve for sensation intensity. However, there are many internal uncertainties in the insect's detection of the stimulus, as well as external measurement uncertainties in behavioral and electrophysiological bioassays. According to signal detection theory, increases in the level of uncertainty will shift the response curve to higher stimulus levels (Green and Swets, 1974). Consequently, we can consider each of the response curves in Figure 5 to represent a curve for sensation intensity that has been shifted to the right by an amount that depends on the external and internal uncertainties. The curve for a single olfactory neuron will be shifted, for example, partly because summation occurs at the central processor. The EAG curve will be shifted because of electrical losses in the antenna that decrease the sensitivity of external measurements.

We can apply the model to two sets of data in Figures 3–5 where EAG and behavioral responses to pheromone were measured. For convenience, consider the horizontal intercept of each response curve to be a type of threshold (although this is not strictly equivalent to T in Eq. 3). According to the model, the EAG thresholds for both *T. ni* and *B. mori* are higher than the behavioral thresholds for pheromone because of differences in the (combined) external and internal uncertainties.

Next, suppose that these relationships hold for other insects. If the activation or the flight response of *H. zea* to *Z*-11 : 16Al correlates with the neurophysiological response in the same way that the behavioral and neurophysiological responses to *Z*-7 : 12Ac correlate in *T. ni*, then the behavioral threshold for *H. zea* should be about 1×10^{-12} μmol/cm^3, the apparent threshold for *T.*

ni. The correlation seems plausible because the measurement procedures and uncertainties are similar. The EAG curve for the queen substance, a sex pheromone component of *A. mellifera* (Kaissling, 1971), is similar to the curve for *T. ni*. Thus, it can be expected that the behavioral response occurs at about 1×10^{-12} μmol/cm^3 also.

Finally, we can apply the idea of sensation to interpretation of the EAG responses to non-pheromonal compounds. In Figure 5, EAGs for non-pheromonal compounds do not begin to occur until much higher concentrations than for pheromones, 1×10^{-6}–1×10^{-4} μmol/cm^3. By analogy with the responses for pheromones, behavioral thresholds for these chemicals perhaps occur at concentrations no lower than two orders of magnitude below the EAG threshold, about 1×10^{-6} μmol/cm^3. The measured behavioral threshold of *A. mellifera* to caproic acid (Schwarz, 1955), AMBC in Figure 5, is in general agreement with such a hypothesis.

Acknowledgments—We thank R.R. Heath for the rubber septum calibration and J.A. Coffelt for assistance with the GLC quantification. We also thank K.E. Matsumoto, J.R. McLaughlin, and R.J. O'Connell for their helpful comments. Mention of a commercial or proprietary product does not constitute an endorsement by the USDA.

REFERENCES

BAKER, T.C., GASTON, L.K., POPE, M. M., KUENEN, L.P.S., and VETTER, R.S. 1981. A high efficiency collection device for quantifying sex pheromone volatilized from female glands and synthetic sources. *J. Chem. Ecol.* 7:961–968.

BAKER, T.C., WILLIS, M.A., HAYNES, K.F., and PHELAN, P.C. 1985. A pulsed cloud of sex pheromone elicits upwind flight in male moths. *Physiol. Entomol.* 10:257–265.

BJÖSTAD, L.B., GASTON, L.K., and SHOREY, H.H. 1980. Temporal pattern of sex pheromone release by female *Trichoplusia ni*. *J. Insect Physiol.* 26:493–498.

BOECKH, J., and BOECKH, V. 1979. Threshold and odor specificity of pheromone-sensitive neurons in the deutocerebrum of *Antheraea pernyi* and *A. polyphemus*. *J. Comp. Physiol.* 132:235–242.

BORST, A. 1984. Identification of different chemoreceptors by electroantennogram recording. *J. Insect Physiol.* 30:507–510.

BROWNLEE, R.G., and SILVERSTEIN, R.M. 1968. A micropreparative gas chromatograph and a modified carbon skeleton determinator. *Anal. Chem.* 40:2077–2079.

BUTLER, L.I., and MCDONOUGH, L.M. 1979. Insect sex pheromones: Evaporation rates of acetates from natural rubber septa. *J. Chem. Ecol.* 5:825–837.

CHARLTON, R.E., and CARDÉ, R.T. 1982. Rate and diel periodicity of pheromone emission from female gypsy moths, *Lymantria dispar* (L.) determined with a glass adsorption collection system. *J. Insect Physiol.* 28:423–430.

ELKINTON, J.S., and CARDÉ, R.T. 1984. Odor dispersion, pp. 73–91, *in* W.J. Bell and R.T. Cardé (eds.). Chemical Ecology of Insects. Sinour Associates, Sunderland, Massachusetts.

ELKINGTON, J.S., CARDÉ, R.T., and MASON, C.J. 1984. Evaluation of time-average dispersion models for estimating pheromone concentration in a deciduous forest. *J. Chem. Ecol.* 10:1081–1108.

FONTA, C., and MASSON, C. 1984. Comparative study by electrophysiology of olfactory responses in bumblebees. *J. Chem. Ecol.* 10:1157–1168.

GREEN, D.M., and SWETS, J.A. 1974. Signal Detection Theory and Psychophysics. Krieger, Huntington, New York.

HEATH, R.R., and TUMLINSON, J.H. 1986. Correlation of retention times on a liquid crystal capillary column with reported vapor pressures and half-lives of compounds used in pheromone formulations. *J. Chem. Ecol.* 12:2081–2088.

HELLAND, I.S., HOFF, J.M., and ANDERBRANT, O. 1984. Attraction of bark beetles (Coleoptera: Scolytidae) to a pheromone trap. Experiment and mathematical models. *J. Chem. Ecol.* 10:723–752.

HIROOKA, Y., and SUWANAI, M. 1976. Role of insect sex pheromone in mating behavior. I. Theoretical consideration on release and diffusion of sex pheromone in the air. *Appl. Entomol. Zool.* 11:126–132.

KAISSLING, K.-E. 1971. Insect olfaction, pp. 351–431, in L.M. Beidler (ed.). Handbook of Sensory Physiology, IV: Chemical Senses 1 Olfaction. Springer-Verlag, Berlin.

MANKIN, R.W., and MAYER, M.S. 1983a. A phenomenological model of the perceived intensity of single odorants. *J. Theor. Biol.* 100:123–138.

MANKIN, R.W., and MAYER, M.S. 1983b. Stimulus–response relationships of insect olfaction: Correlations among neurophysiological and behavioral measures of response. *J. Theor. Biol.* 100:613–630.

MANKIN, R.W., and MAYER, M.S. 1984. The insect antenna is not a molecular sieve. *Experientia* 40:1251–1252.

MANKIN, R.W., VICK, K.W., MAYER, M.S., and COFFELT, J.A. 1980. Anemotactic response threshold of the Indian meal moth, *Plodia interpunctella* (Hübner) (Lepidoptera: Pyralidae) to its sex pheromone. *J. Chem. Ecol.* 6:919–928.

MANKIN, R.W., VICK, K.W., COFFELT, J.A., and WEAVER, B.A. 1983. Pheromone-mediated flight by male *Plodia interpunctella* (Hübner) (Lepidoptera: Pyralidae). *Environ. Entomol.* 12:1218–1222.

MAYER, M.S. 1968. Response of single olfactory cell of *Triatoma infestans* to human breath. *Nature* 220:924–925.

MAYER, M.S. 1973. Attraction studies of male *Trichoplusia ni* (Lepidoptera: Noctuidae) with new combination of olfactometer and pheromone dispenser. *Ann. Entomol. Soc. Am.* 66:1101–1196.

MAYER, M.S., and MANKIN, R.W. 1985. Neurobiology of pheromone perception, pp. 95–144, *in* G.A. Kerkut and L.I. Gilbert (eds.). Comprehensive Insect Physiology, Biochemistry and Pharmacology, Vol. 9, Behaviour. Pergamon Press, Oxford, England.

MAYER, M.S., MANKIN, R.W., and LEMIRE, G.F. 1984. Quantitation of the insect electroantennogram: measurement of sensillar contributions, elimination of background potentials, and relationship to olfactory sensation. *J. Insect Physiol.* 30:757–763.

O'CONNELL, R.J., KOCSIS, W.A., and SCHOENFELD, R.L. 1973. Minicomputer identification and timing of nerve impulses mixed in a single recording channel. *Proc. IEEE* 61:1615–1621.

OLSSON, A.M., JÖNSSON, J.A., THELIN, B., and LILJEFORS, T. 1983. Determination of the vapor pressures of moth sex pheromone components by a gas chromatographic method. *J. Chem. Ecol.* 9:375–385.

SCHWARZ, R. 1955. Über die Reichschärfe der Honigbie. *Z. vergl. Physiol.* 37:180–210.

SOWER, L.L., and FISH, J.C. 1975. Rate of release of the sex pheromone of the female Indian meal moth. *Environ. Entomol.* 4:168–169.

SOWER, L.L., GASTON, L.K., and SHOREY, H.H. 1971. Sex pheromones of noctuid moths 26. Female release rate, male response threshold, and communication distance of *T. ni*. *Ann. Entomol. Soc. Am.* 64:1448–1456.

STEVENS, S.S. 1975. Psychophysics. John Wiley & Sons, New York.

TULLY, J.C., and CARDILLO, M.J. 1984. Dynamics of molecular motion at single-crystal surfaces. *Science* 223:445–450.

VENARD, R., and PICHON, Y. 1981. Etude électro-antennographique de la reponse périphérique de l'antenne de *Drosophila melanogaster* à des stimulations odorants. *C.R. Acad. Sci. Paris* 293:839–842.

VENARD, R., and PICHON, Y. 1984. Electrophysiological analyses of the peripheral response to odors in wild type and smell deficient OLF C mutant of *Drosophila melanogaster*. *J. Insect Physiol.* 30:1–5.

WADHAMS, L.J. 1982. Coupled gas chromatography-single cell recording: A new technique for use in the analysis of insect pheromones. *Z. Naturforsch.* 37c:947–952.